K^-/K^+ ratios in relativistic heavy-ion collisions

G.Q. Li and G.E. Brown
Department of Physics and Astronomy, State University of New York at Stony Brook, Stony Brook, New York 11794

We study K^-/K^+ ratios as a function of centrality (participant nucleon number), transverse mass (m_t), and rapidity, in heavy-ion collisions at beam energies between 1A and 2A GeV. We use the relativistic transport model that includes expicitly the strangeness degrees of freedom and consider two scenarios for kaon properties in dense matter, one with and one without medium modifications of their properties. In both scenarios, The K^-/K^+ ratio does not change very much with the centrality, while the K/π and $\bar{K}/\pi$ ratios increase with increasing centrality. Significant differences are predicted, both in magnitudes and shapes, for the m_t spectra and rapidity distributions of K^-/K^+ ratio. Experimental measurement of these ratios, currently under investigation by the FOPI, KaoS, E866, and E895 collaborations, will be useful in revealing the kaon in-medium properties.

25.75.Dw, 26.60.+c, 24.10.Lx

I. INTRODUCTION

Whether and how hadronic properties, such as their masses, widths, and dispersion relations, are modified in hot and dense medium is a topic of great current interest. Of particular importance are the medium modifications of kaon properties, as they are related to both spontaneous and explicit chiral symmetry breaking, and they are useful inputs for the study of kaon condensation and neutron star properties [1,2]. Since the pioneering work of Kaplan and Nelson [3] on the possibility of kaon condensation in nuclear matter, a huge amount of theoretical effort has been devoted to the study of kaon properties in dense matter, using such diversified approaches as chiral perturbation theory [4–12], the Nambu−Jona-Lasinio model [13], and SU(3) Walecka-type mean-field model [14,15]. Although quantitatively results from these different models are not identical, qualitatively, a consistent picture has emerged; namely, in nuclear matter the K^+ feels a weak repulsive potential, whereas the K^- feels a strong attractive potential.

Experimentally, in-medium properties of kaon and antikaon can be obtained from the analysis of kaon-nucleus scattering [16,17] and kaonic atom data [18]. The information so obtained is, unfortunately, restricted to low densities. For the study of kaon condensation, densities much higher than that accessible by kaonic atoms are involved. This can only be obtained by analysing heavy-ion collision data on various observables involving kaon and antikaon. Measurements of kaon spectra and flow have been systematically carried out in heavy-ion collisions at SIS (1-2 AGeV), AGS (10 AGeV), and SPS (200 AGeV) energies [19]. The analysis of their yields, spectra, and in particular collective flow has indeed provided useful information about kaon properties in dense nuclear matter [20–28]. So far most of the experimental data from the FOPI [29–31] and KaoS [32–35] collaborations at SIS/GSI seem to be consistent with the predictions from the chiral perturbation theory.

To put these conclusions on a firmer footing, additional observables and experimental data from independent collaborations will certainly be useful. In this paper we study the centrality, transverse mass (m_t), and rapidity dependence of the K^-/K^+ ratio in heavy-ion collisions. Since the medium effects act oppositely on kaon and antikaon, their ratio can reflect more precisely these effects, as was pointed out in Refs. [36,37]. We will consider Ni+Ni, Ru+Ru and Au+Au collisions at beam energies between 1 and 2A GeV. These systems are being investigated by the FOPI [38] and KaoS [39] collaborations at SIS/GSI. Furthermore, the Au+Au collisions are also being analysed by the E866 [36,37] and E895 [40,41] collaborations at the AGS/BNL.

This paper is arranged as follows. In Section II, we briefly review the relativistic transport model, kaon in-medium properties and elementary kaon production cross sections. The results are presented in Section III. The paper ends with a short summary in Section IV.

II. THE RELATIVISTIC TRANSPORT MODEL AND KAON PRODUCTION

Heavy-ion collisions involve very complicated nonequilibrium dynamics. One needs to use transport models in order to extract from experimental data the information about in-medium properties of hadrons. In this work we will use the relativistic transport model similar to that developed in Ref. [42]. Instead of the usual linear and non-linear σ-ω models, we base our model on the effective chiral Lagrangian recently developed by Furstahl, Tang, and Serot [43], which is derived using dimensional analysis, naturalness arguments, and provides a very good description of nuclear matter and finite nuclei. In the mean-field approximation, the energy density for the general case of asymmetric nuclear matter is given by

$$\varepsilon_N = \frac{2}{(2\pi)^3}\int_0^{K_{fp}} d\mathbf{k}\sqrt{\mathbf{k}^2+m_N^{*2}} + \frac{2}{(2\pi)^3}\int_0^{K_{fn}} d\mathbf{k}\sqrt{\mathbf{k}^2+m_N^{*2}}$$

$$+ W\rho + R\frac{1}{2}(\rho_p - \rho_n) - \frac{1}{2C_V^2}W^2 - \frac{1}{2C_\rho^2}R^2 + \frac{1}{2C_S^2}\Phi^2$$
$$+ \frac{S'^2}{4C_S^2}d^2\left\{\left(1-\frac{\Phi}{S'}\right)^{4/d}\left[\frac{1}{d}\ln\left(1-\frac{\Phi}{S'}\right)-\frac{1}{4}\right]+\frac{1}{4}\right\}$$
$$- \frac{\xi}{24}W^4 - \frac{\eta}{2C_V^2}\frac{\Phi}{S'}W^2. \quad (1)$$

The nucleon effective mass m_N^* is related to its scalar field Φ by $m_N^* = m_N - \Phi$. W and R are the isospin-even and isospin-odd vector potentials, respectively. The last three terms give the self-interactions of the scalar field, the vector field, and the coupling between them. The meaning and values of various parameters in Eq. (1) can be found in [43].

From the energy density of Eq. (1), we can also derive a relativistic transport model for heavy-ion collisions. At SIS energies, the colliding system consists mainly of nucleons, delta resonances, and pions. While medium effects on pions are neglected, nucleons and delta resonances propagate in a common mean-field potential according to the Hamilton equation of motion,

$$\frac{d\mathbf{x}}{dt} = \frac{\mathbf{p}^*}{E^*}, \quad \frac{d\mathbf{p}}{dt} = -\nabla_x(E^* + W), \quad (2)$$

where $E^* = \sqrt{\mathbf{p}^{*2} + m^{*2}}$. These particles also undergo stochastic two-body collisions, including both elastic and inelastic scattering.

In heavy-ion collisions at incident energies considered in this work, kaons can be produced from pion-baryon and baryon-baryon collisions. For the former we use cross sections obtained in the resonance model by Tsushima *et al.* [44]. For the latter the cross sections obtained in the one-boson-exchange model of Ref. [45,46] are used. Both models describe the available experimental data very well. For antikaon production from pion-baryon collisions we use the parameterization proposed by Sibirtsev *et al.* [47]. For baryon-baryon collisions, we use a somewhat different parameterization, which describes the experimental data better, than Ref. [47]. In addition, the antikaon can also be produced from strangeness-exchange processes such as $\pi Y \to \bar{K}N$ where Y is either a Λ or Σ hyperon. The cross sections for these processes are obtained from the reverse ones, $\bar{K}N \to \pi Y$, by the detailed-balance relation. All the parameterizations for the elementary cross sections and comparisons with experimental data can be found in our recent paper [28].

Particles produced in elementary hadron-hadron interactions in heavy-ion collisions cannot escape the environment freely. Instead, they are subjected to strong final-state interactions. For the kaon, because of strangeness conservation, its scattering with nucleons at low energies is dominated by elastic and pion production processes, which do not affect its final yield but changes its momentum spectra. The final-state interaction for the antikaon is much stronger. Antikaons can be destroyed in the strangeness-exchange processes. They also undergo elastic scattering. Both the elastic and absorption cross sections increase rapidly with decreasing antikaon momenta. This will have strong effects on the final K^- momentum spectra in heavy-ion collisions.

we will consider two scenarios for kaon properties in nuclear medium, one with and one without medium modification. From the chiral Lagrangian the kaon and antikaon in-medium energies can be written as [28]

$$\omega_K = \left[m_K^2 + \mathbf{k}^2 - a_K\rho_S + (b_K\rho)^2\right]^{1/2} + b_K\rho \quad (3)$$

$$\omega_{\bar{K}} = \left[m_K^2 + \mathbf{k}^2 - a_{\bar{K}}\rho_S + (b_K\rho)^2\right]^{1/2} - b_K\rho \quad (4)$$

where $b_K = 3/(8f_\pi^2) \approx 0.333$ GeVfm^3, a_K and $a_{\bar{K}}$ are two parameters that determine the strength of the attractive scalar potential for kaon and antikaon, respectively. If one considers only the Kaplan-Nelson term, then $a_K = a_{\bar{K}} = \Sigma_{KN}/f_\pi^2$. In the same order, there is also the range term which acts differently on kaon and antikaon, and leads to different scalar attractions. Since the exact value of Σ_{KN} and the size of the higher-order corrections are still under intensive debate, we take the point of view that $a_{K,\bar{K}}$ can be treated as free parameters and try to constrain them from the experimental observables in heavy-ion collisions. In Ref. [27,28] we found that $a_K \approx 0.22$ GeV^{2}fm^3 and $a_{\bar{K}} \approx 0.45$ GeV^{2}fm^3 provide a good description of kaon and antikaon spectra in Ni+Ni collisions at 1A and 1.8A GeV. These values will be used in this work as well.

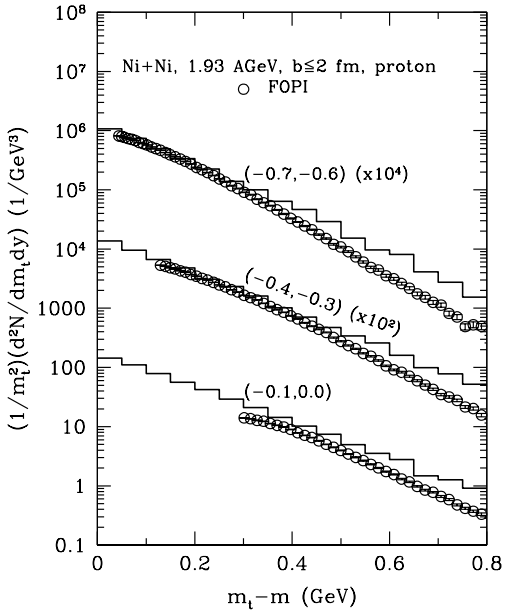

FIG. 1. Proton transverse mass spectra in central Ni+Ni collisions at 1.93 AGeV in three rapidity bins. The open circles are experimental data from the FOPI collaboration [48,49].

In nuclear medium, kaon and antikaon masses are modified, so are their production thresholds. We will then use $\sqrt{s_0^*}$, which are calculated with effective masses, in evaluating the in-medium production cross sections. This amounts to the change of threshold, or approximately, to the change of available phase space. In addition to the change in the production cross sections, the medium effects on kaon and antikaon also affect their momentum spectra, when they propagate in the mean-field potentials. The Hamilton equations of motion for kaon and antikaon are very similar to those for nucleons [21],

$$\frac{d\mathbf{r}}{dt} = \frac{\mathbf{k}}{\omega_{K,\bar{K}} \mp b_k \rho_N}, \quad \frac{d\mathbf{k}}{dt} = -\nabla_x U_{K,\bar{K}}, \tag{5}$$

where the minus sign corresponds to kaon, and the plus sign to antikaon. It is clearly that the K^+ momentum increases and that of K^- decreases when they propagate in their respective mean field potentials. This affects significantly their momentum spectra, and especially the momentum spectra of their ratio.

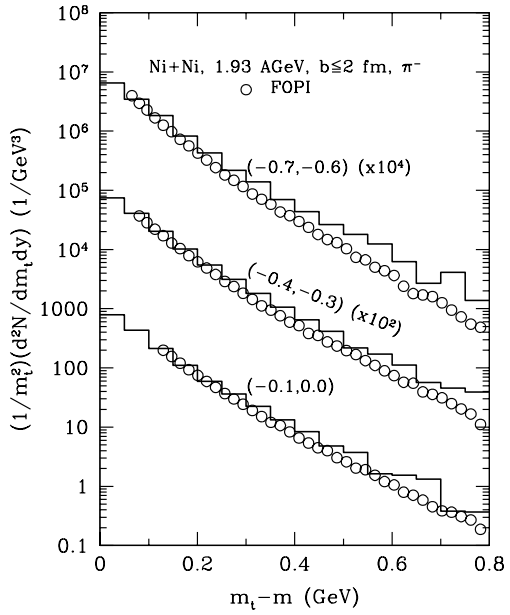

FIG. 2. Same as Fig. 1, for π^-.

III. RESULTS AND DISCUSSIONS

In this section we present our results for the centrality, transverse mass, and rapidity dependences of K^-/K^+ ratio. Before that, we first compare the proton and pion m_t spectra from our calculation with the available experimental data, taking central Ni+Ni collisions at 1.93A GeV as an example. In Fig. 1 we compare the proton transverse mass spectra in three rapidity bins with the experimental data from the FOPI collaboration [48,49]. Similar comparison for the π^- transverse mass spectra is shown in Fig. 2. Our results are seen to be in good agreement with the data [48,49]. Similarly, in Ref. [28] the proton and π^- rapidity distributions obtained in our transport model were shown to be in good agreement with the FOPI data.

A. centrality dependence

In this subsection, we discuss the centrality dependence of the K^-/K^+ ratio. We use the participant nucleon number A_{part} as the measurement of the centrality. In Fig. 3 we show the A_{part} dependence of the pion multiplicity in Ni+Ni collisions at 1.93A GeV. The solid line gives 1/3 of the total pion number obtained in our calculation, while the circles and squares are the FOPI data [50] for π^- and π^+, respectively. It is seen that our results are in good agreement with the data, and that the pion multiplicity increases almost linearly with the participant nucleon number. In other words, the N_π/A_{part} ratio is almost independent of the centrality.

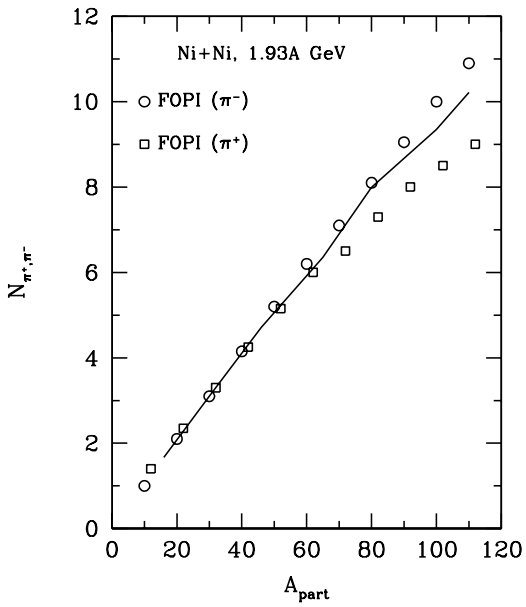

FIG. 3. Pion multiplcity as a function of the participant nucleon number in Ni+Ni collisions at 1.93 AGeV.

On the other hand, it is well-known that the K^+ (usually shown in terms of K^+/π^+ ratio) yield increases more than linearly with the A_{part} for beam energies ranging from 1A GeV [32–34,46] to 10A GeV [36,51]. Our results for K/π and $\bar{K}/\pi$ ratios in Au+Au collisions are shown in Fig. 4. It is seen that either with or without kaon medium effects, these ratios increase more than linearly

with the participant nucleon number. This is due to the increasing importance of the secondary processes involving baryon-resonances, pions, and hyperons in the case of antikaon production, when going from peripheral to central collisions. The E866 data for Au+Au collisions at 11.6A GeV/c indicate that K^-/π^+ ratio also increases with increasing centrality [51].

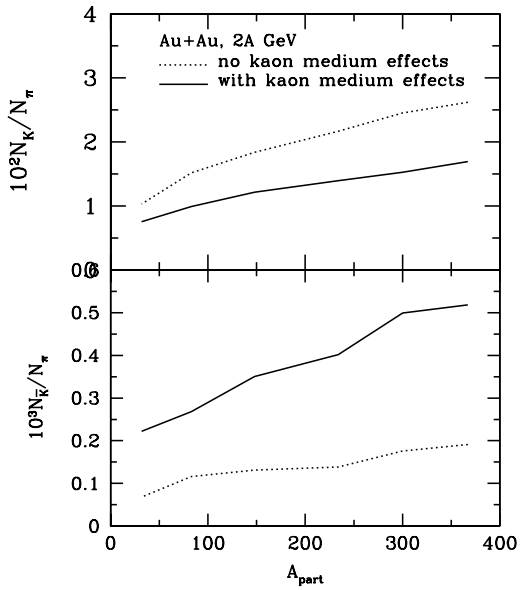

FIG. 4. K/π and $\bar{K}/\pi$ ratios as a function of the participant nucleon number in Au+Au collisions at 2A GeV.

The centrality dependence of the K^-/K^+ ratios is shown in Figs. 5, 6, and 7, for Ni+Ni at 1.8A GeV, Ru+Ru at 1.69A GeV, and Au+Au at 2A GeV, respectively. For Ni+Ni collisions, we also shown in Fig. 5 the experimental data from the KaoS collaboration [35] by open circles. For all the systems considered, it is seen that either with or without medium effects, the K^-/K^+ ratio does not depend very much on the centrality, since in both scenarios, the K/π and $\bar{K}/\pi$ ratios increase at about the same rate with increasing centrality (see Fig. 4). The experimental data of the KaoS collaboration for Ni+Ni collisions (Fig. 5) show little increase of the ratio towards central collisions within their statistical uncertainties. Preliminary data from the FOPI collaboration for Ru+Ru at 1.69A GeV [52], and data from E866 collaboration for Au+Au collisions at 10.6A GeV [36] both show weak centrality dependence for the K^-/K^+ ratio.

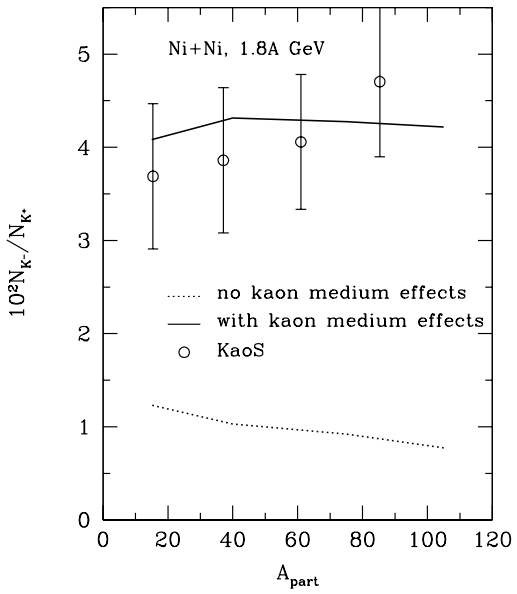

FIG. 5. K^-/K^+ ratio as a function of the participant nucleon number in Ni+Ni collisions at 1.8A GeV. The open circles are the experimental data from the KaoS collaboration [35]

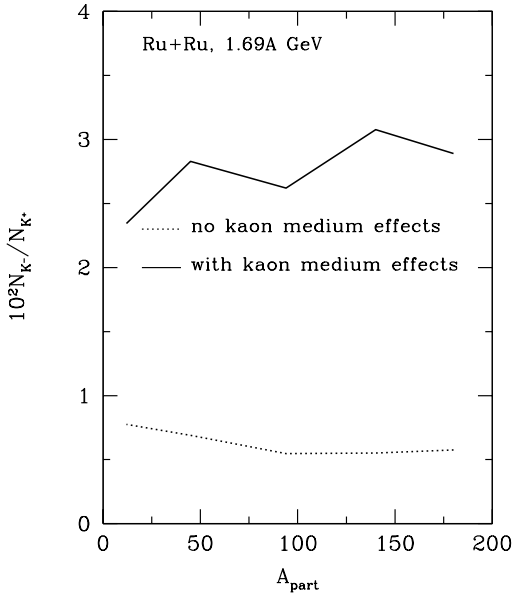

FIG. 6. Same as Fig. 5, for Ru+Ru collisions at 1.69A GeV.

Without kaon medium effects, the K^-/K^+ ratio ranges from 0.006 in Ru+Ru at 1.69A GeV, to 0.01

in Ni+Ni collisions at 1.8A GeV, to 0.0075 in Au+Au collisions at 2A GeV. The increase of this ratio from Ru+Ru to Ni+Ni comes from the increase in beam energy, since at these energies the antikaon excitation function is steeper than that of kaon because of a higher threshold. On the other, the decrease of this ratio from Ni+Ni to Au+Au is due to the fact that in the large Au+Au system the antikaon absorption effects become more significant. Qualitatively, the absorption probability is proportional to the product of the absorption cross section and the average size of the system. In this case the experimental data from the KaoS collaboration for Ni+Ni collisions are significantly underestimated (see Fig. 5).

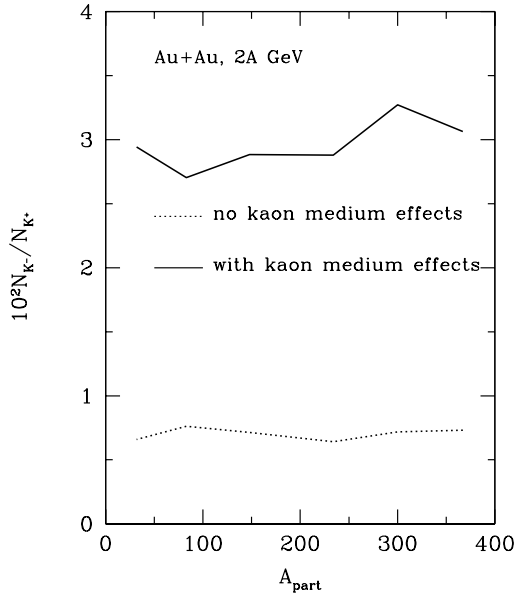

FIG. 7. Same as Fig. 5, for Au+Au collisions at 2A GeV.

When kaon medium effects are included, the K^-/K^+ ratio increase by about a factor of 4, for all the systems considered here. This increase results from a factor of 3 increase in antikaon yield and about 35% reduction in kaon yield. In this case, the K^-/K^+ ratio from the KaoS collaboration can be nicely explained. Furthermore, preliminary data from the FOPI collaboration indicate a K^-/K^+ ratio of about 0.02-0.03 in Ru+Ru collisions at 1.69A GeV. Our predictions that include kaon medium effects are seen to be in better agreement with these preliminary data than those without the kaon medium effects.

Naively, it is expected that when kaon medium effects are included, the K^-/K^+ ratio should increase with the increasing centrality, since in central collisions reduction of the antikaon mass and the increase of kaon mass are the most significant. However, since the second processes $Y\pi \to \bar{K}N$ play an important role in antikaon production, and hyperon yield, which are produced in association with kaons, is reduced most significantly in central collisions, the increase in the reduction of antikaon mass towards central collisions is largely compensated. The increase of the K^-/K^+ ratio with increasing centrality when kaon medium effects are included is thus marginal (on the order of 10-20%).

It is also of interest to show the beam energy dependence of the K^-/K^+ ratio in central Au+Au collisions. This is done in Fig. 8 for impact parameter b= 1 fm. In both scenarios with and without kaon medium effects, the ratio is seen to increase as beam energy increases. This is understandable, as the antikaon production threshould is higher than that of kaon, so at these energies, the antikaon production cross sections increases faster than that of kaon.

Finally, we show in Fig. 9 the time evolution of central density, kaon yield, and antikaon yield in Au+Au collisions at 1.5A GeV and b=3 fm. It is seen that for a considerable duration of time the system is compressed to a density of around $3\rho_0$, and during this period of time, most of the kaons and antikaons are produced. As was shown in Ref. [28], K^- condensation is predicted to occur around three times normal nuclear matter based on current theoretical and empirical information. The experimental data on kaon and antikaon yields, spectra, ratios, and flow from Au+Au collisions at 1.5A Gev will be very useful in pinning down the critical density for kaon condensation.

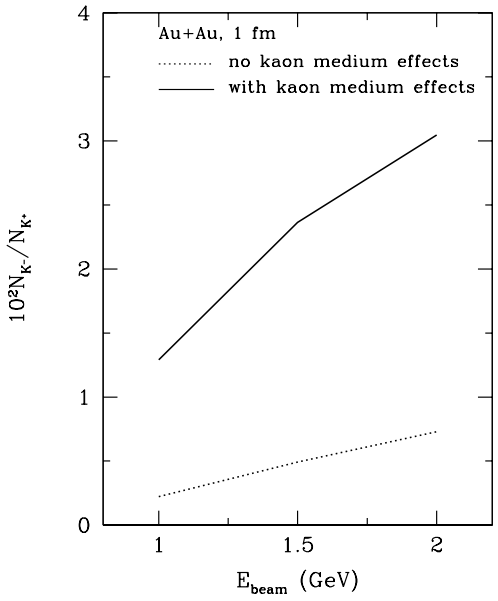

FIG. 8. Beam energy dependence of K^-/K^+ ratio in central Au+Au collisions.

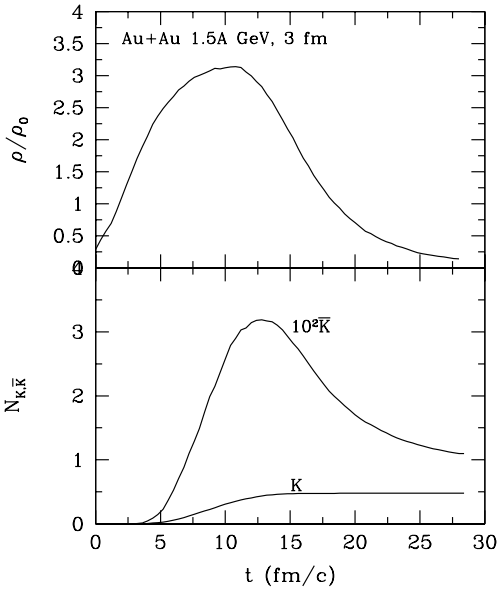

FIG. 9. Time evolution of central density as well as kaon and antikaon yields in Au+Au collisions at 1.5A GeV and 3 fm.

B. Transverse mass spectra

The effects of kaon and antikaon mean-field potentials can be more clearly seen by looking at their ratio as a function of their tranverse mass (or kinetic energy). The results are shown in Figs. 10, 11, 12, and 13, for Ni+Ni at 1.8A GeV, Ru+Ru at 1.69A GeV, Au+Au at 1.5A GeV, and Au+Au at 2A GeV, respectively. The results for Ni+Ni are presented in terms of kinetic energy for minimum-biased collisions, in accordance with the experimental data from the KaoS collaboration [35], shown in Fig. 10 with open circles.

When kaon medium effects are neglected, the K^-/K^+ ratio is seen to increase slightly with increasing transverse momentum. Since the antikaon absorption cross section by nucleons becomes large at low momentum, low-momentum antikaons are more strongly absorbed than high-momentum ones. This makes the K^-/K^+ ratio decrease at small transverse mass. When medium effects are included, we find that the shape of the K^-/K^+ ratio is completely different from that without kaon medium effects. The ratio is now seen to increase dramatically towards small transverse mass. For example, for Ru+RU collisions, it increases from about 0.02 at $m_t - m_K = 0.3$ GeV to about 0.08 when $m_t - m_K$ approaches zero. The difference in the shape of the m_t spectra comes from the propagation of kaons and antikaons in their mean-field potential. Kaons are 'pushed' to high momenta by the repulsive potential, while antikaons are 'pulled' to low momenta, leading to an enhanced K^-/K^+ ratio at small transverse masses. From Fig. 10, we also see that the effects of propagation in mean-field potentials are more pronounced in central collisions.

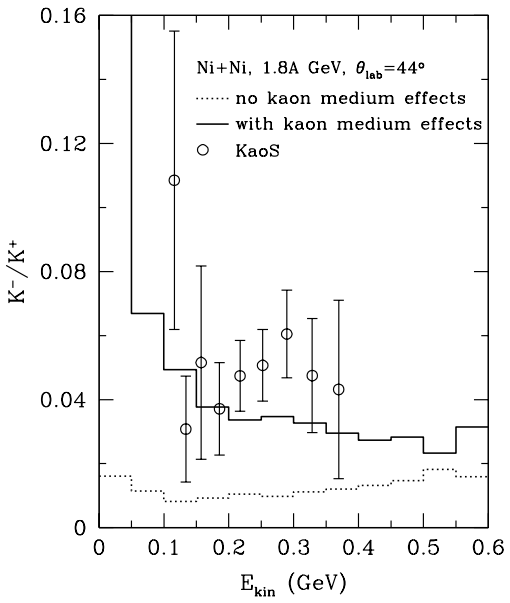

FIG. 10. Kinetic energy spectra of the K^-/K^+ ratio in Ni+Ni collisions at 1.8A GeV. The experimental data are from the KaoS collaboration [35]

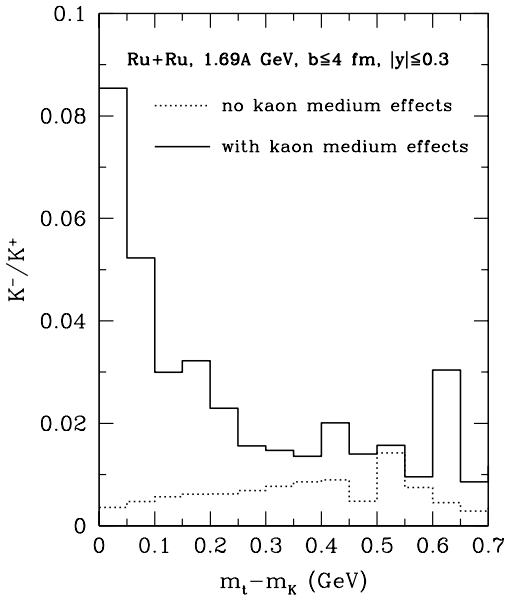

FIG. 11. Transverse mass spectra of K^-/K^+ ratio in central Ru+Ru collisions at 1.69A GeV.

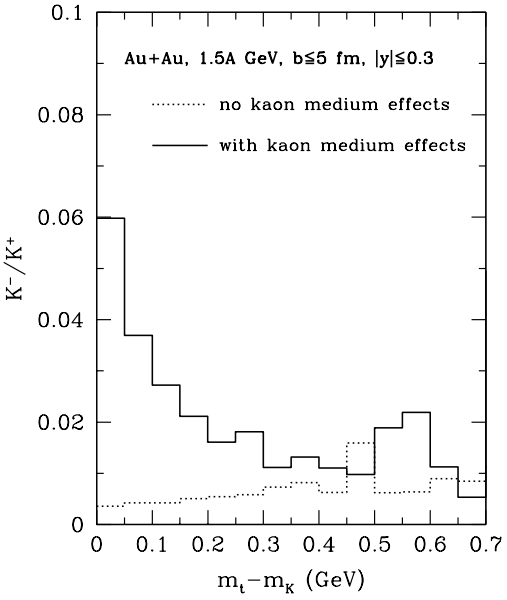

FIG. 12. Same as Fig. 11, for Au+Au collisions at 1.5A GeV.

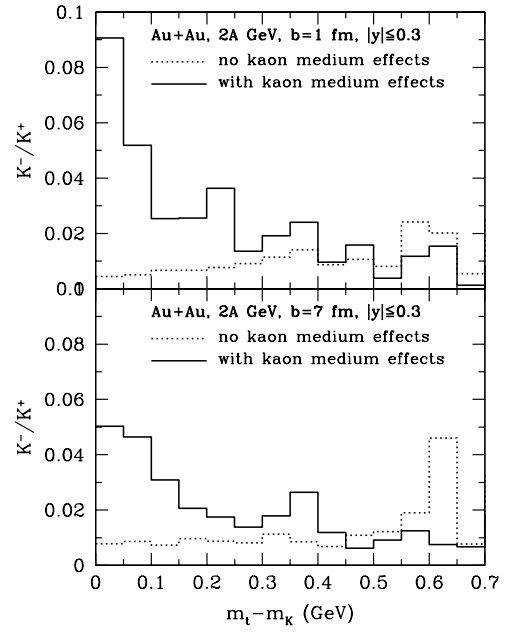

FIG. 13. Same as Fig. 11, for Au+Au collisions at 2A GeV.

Experimental data from the KaoS collaboration provided some indication for this dramatic increase of the K^-/K^+ ratio at small momenta [35]. Our results are compared with these data in Fig. 10. It is seen that our results including the kaon medium effects are in much better agreement with the data. Of course the statistical uncertainty of the data is still quite large (especially for the first datum point at 0.12 GeV). This will be improved in their recent analysis of Ni+Ni collisions at 1.93A GeV [39]. It will also be very useful if the ratio at kientic energies less than 0.1 GeV can be measured experimentally.

It should be emphasized that in this work, as in our previous study of kaon production in heavy-ion collisions, the explicit momentum dependence of the kaon scalar and vector potential is not considered. This should be a reasonable approximation for heavy-ion collisions at 1-2A GeV, as kaons (antikaon) produced in these reactions usually have small momenta. This approximation will break down at higher beam energies about 10A GeV. A recent theoretical calculation [53] indicated that the attractive antikaon potential becomes weaker as its momentum (relative to the medium) increases. Experimental data on K^--nucleus scattering at high incident momenta also indicate a repulsive (rather than an attractive) antikaon optical-model potential. This momentum dependence of the kaon (antikaon) potential might explain the fact that so far the experimental data for heavy-ion collisions at 10A GeV do not show substantial enhancement of the K^-/K^+ ratio approaching small transverse masses (momenta).

C. Rapidity distribution

The rapidity distributions of the K^-/K^+ ratio should provide quite similar information on kaon medium effects as its transverse mass spectra. The results for Ni+Ni at 1.93A Gev, Ru+Ru at 1.69A GeV, Au+Au at 1.5A GeV, and Au+Au collisions are shown in Figs. 14, 15, 16, and 17, respectively. For Ni+Ni collisions we show also the preliminary data from the FOPI collaboration [52,54] by circles.

Indeed, the magnitudes and the shapes of these rapidity distributions with and without kaon medium effects are very different. Without kaon medium effects, the rapidity distribution is seen to decrease slightly from target/projectile rapidities to mid-rapidity. This is again due to the large absorption cross section for slow-moving antikaons. When kaon medium effects are included, there appears not only an overall increase of the ratio, because of the increased production cross section of antikaons, but also a significant change of the shape of the rapidity distribution. The K^-/K^+ ratio is seen to increase steadily from target/projectile rapidities to mid-rapidity. Our results with kaon medium effects are in much better agreement with the preliminary data from the FOPI collaboration (Fig. 14).

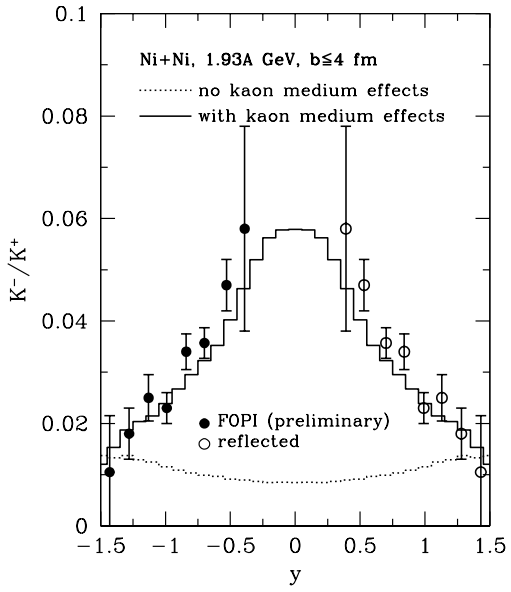

FIG. 14. Rapidity distribution of K^-/K^+ ratio in central Ni+Ni collisions at 1.93A GeV. The solid circles are preliminary experimental data from the FOPI collaboration [52,54], while the open circles are obtained by reflecting the data with respect to the mid-rapidity.

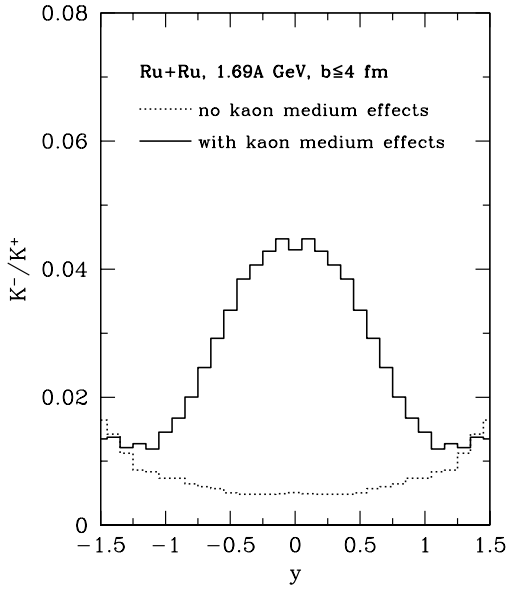

FIG. 15. Same as Fig. 14, for Ru+Ru collisions at 1.69A GeV.

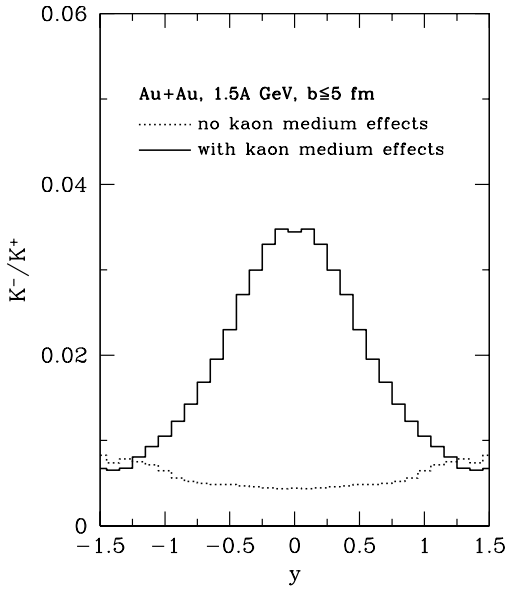

FIG. 16. Same as Fig. 14, for Au+Au collisions at 1.5A GeV.

For Au+Au collisions at 2A GeV and $b = 1$ fm, we also show in the figure the K^-/K^+ ratio before any final-state interactions on kaons and antikaons are included, which means that even the antikaon absorption is turned off. We see that in this case, the ratio also decreases from mid-rapidity to projectile and target rapidities. The decrease of this ratio towards large rapidities (momenta) reflects the fact that antikaons are produced at a higher threshold than kaons, so that their momentum distributions are restricted more severely by the available energies. However, we need to emphasize that antikaon absorption and the fact that its absorption cross section increases at low momenta are well-known experimental facts and must be included in transport model calculations.

As mentioned in the Introduction, so far most of the experimental data from the FOPI and KaoS collaborations at SIS/GSI are consistent with the chiral perturbation theory predictions for kaon in-medium properties. For an ultimate confirmation of these medium effects, it should be be very useful if independent experimental data for Au+Au collisions at 2A GeV from the E866 and E895 collaborations could become available.

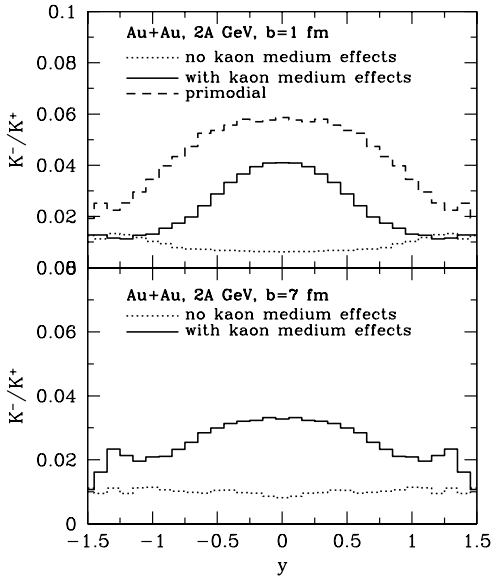

FIG. 17. Same as Fig. 14, for Au+Au collisions at 2A GeV.

IV. SUMMARY

In summary, we studied K^-/K^+ ratios as a function of centrality (participant nucleon number), transverse mass (m_t), and rapidity, in Ni+Ni, Ru+Ru, and Au+Au collisions at beam energies between 1 and 2A GeV. We used the relativistic transport model that includes explicitly the strangeness degrees of freedom and considered two scenarios for kaon properties in dense matter, one with and one without medium modifications of their properties. In both scenarios, The K^-/K^+ ratio does not change very much with the centrality, while the K/π and $\bar{K}/\pi$ ratios increase with increasing centrality. Significant differences were predicted, both in magnitudes and shapes, for the m_t spectra and rapidity distributions of K^-/K^+ ratio. We found that the experimental data from the KaoS collaboration for the kinetic energy spectra of the K^-/K^+ ratio and those from the FOPI collaboration for its rapidity distribution support the suggestion of kaon medium effects. We emphasize that the independent data from the E866 and E895 collaborations for Au+Au collisions at 2A GeV will be useful in confirming or confronting these findings.

We are grateful to N. Herrmann and P. Senger for sending us the data files, and to N. Herrmann, C. Ogilvie, and P. Senger for useful communications. This work is supported in part by the Department of Energy under Grant No. DE-FG02-88ER40388.

[1] G.E. Brown, K. Kubodera, D. Page, and P. Pizzecherro, Phys. Rev. D 37 (1988) 2042.
[2] V. Thorsson, M. Prakash, and J. M. Lattimer, Nucl. Phys. A572 (1994) 693.
[3] D.B. Kaplan and A.E. Nelson, Phys. Lett. **B175**, 57 (1986).
[4] G.E. Brown, K. Kubodera, and M. Rho, Phys. Lett. 192B (1987) 272.
[5] H.D. Politzer and M.B. Wise, Phys. Lett. 273B (1991) 156.
[6] G.E. Brown, C.-H. Lee, M. Rho, and V. Thorsson, Nucl. Phys. A567 (1994) 937.
[7] C.-H. Lee, G.E. Brown, D.P. Min, and M. Rho, Nucl. Phys. A585 (1995) 401.
[8] N. Kaiser, P.B. Siegel, and W. Weise, Nucl. Phys. 594 (1995) 325.
[9] T. Waas, N. Kaiser, and W. Weise, Phys. Lett. B379 (1996).
[10] C.-H. Lee, Phys. Rep 275 (1996) 255.
[11] N. Kaiser, T. Waas, and W. Weise, Nucl. Phys. A612 (1997) 297.
[12] T. Waas and W. Weise, Nucl. Phys. A625 (1997) 287.
[13] M. Lutz, A. Steiner, and W. Weise, Nucl. Phys. A574 (1994) 755.
[14] J. Schaffner, A. Gal, I.N. Mishistin, H. Stöcker, and W. Greiner, Phys. Lett. B334 (1994) 268.
[15] R. Knorren, M. Prakash, and P. J. Ellis, Phys. Rev. C52 (1995) 3470.
[16] G.E. Brown, C.B. Dover, P.B. Siegel, and W. Weise, Phys. Rev. Lett. 60 (1988) 2723.
[17] E. Friedman, A. Gal, and J. Mares, Nucl. Phys. **A625** (1997) 272.
[18] E. Friedman, A. Gal, and C. J. Batty, Nucl. Phys. A579 (1994) 518.
[19] See e.g., QM'95, Nucl. Phys. A590 (1995); QM'96, Nucl. Phys. A610 (1996).
[20] G. Q. Li, C. M. Ko, and B. A. Li, Phys. Rev. Lett. 74 (1995) 235.
[21] G. Q. Li and C. M. Ko, Nucl. Phys. A594 (1995) 460.
[22] G.Q. Li and C.M. Ko, Phys. Rev. C54 (1996) R2159.
[23] W. Cassing, E. L. Bratkovskaya, U. Mosel, S. Teis, and A. Sibirtsev, Nucl. Phys. A614 (1997) 415.
[24] E.L. Bratkovskaya, W. Cassing, and U. Mosel, Nucl. Phys. A622 (1997) 593.
[25] Z.S. Wang, A. Faessler, C. Fuchs, V.S. Uma Maheswari, and D.S. Kosov, Phys. Rev. Lett. 79 (1997) 4096.
[26] Z.S. Wang, A. Faessler, C. Fuchs, V.S. Uma Maheswari, and D.S. Kosov, Nucl. Phys. A628 (1998) 151.
[27] G.Q. Li, C.-H. Lee, and G.E. Brown, Phys. Rev. Lett. **79** (1997) 5214.
[28] G.Q. Li, C.-H. Lee, and G.E. Brown, Nucl. Phys A625 (1997) 372.
[29] J.L. Ritman *et al.* (FOPI collaboration), Z. Phys. A352 (1995) 355.
[30] N. Herrmann for the FOPI collaboration, Nucl. Phys. A610 (1996) 49c.
[31] D. Best *et al.* (FOPI collaboration), Nucl. Phys. A625 (1997) 307.
[32] D. Miskowiec *et al.* (KaoS collaboration), Phys. Rev. Lett. **72** (1994) 3650.

[33] R. Elmer *et al.* (KaoS collaboration), Phys. Rev. Lett. 77 (1996) 4886.
[34] P. Senger for the KaoS collaboration, Heavy Ion Physics **4** (1996) 317.
[35] R. Barth *et al.* (KaoS collaboration), Phys. Rev. Lett. 78 (1997) 4027.
[36] C. Ogilvie, J. Phys. G **23** (1997) 1803.
[37] C. Ogilvie, Nucl. Phys. A630 (1998) 571c
[38] N. Herrmann, private communications
[39] P. Senger, private communications.
[40] M. Justice *et al.* (EOS collaboration), nucl-ex/9708005.
[41] D. Best for the E895 collaboration, J. Phys. G **23** (1997) 1873.
[42] C.M. Ko, Q. Li, and R. Wang, Phys. Rev. Lett. **59** (1987) 1084.
[43] R.J. Furnstahl, H.-B. Tang, and B.D. Serot, Phys. Rev. C 52 (1995) 1368.
[44] K. Tsushima, S.W. Huang, and A. Faessler, Phys. Lett. B337 (1994) 245; J. Phys. G 21 (1995) 33.
[45] G.Q. Li and C.M. Ko, Nucl. Phys. A594 (1995) 439.
[46] G.Q. Li, C.M. Ko, and W.S. Chung, Phys. Rev. C 57 (1998).
[47] A. Sibirtsev, W. Cassing, and C.M. Ko, Z. Phys. A 358 (1997) 101.
[48] B. Hong *et al.* (FOPI collaboration), Phys. Lett. B **407** (1997) 115.
[49] B. Hong *et al.,* (FOPI collaboration), Phys. Rev. C 57 (1998) 244.
[50] D. Pelte *et al.* (FOPI collaboration), Z. Phys. A 359 (1997) 55.
[51] L. Ahle *et al.,* (E866 collaboration), Nucl. Phys. A610 (1996) 139c.
[52] Y. Leifels, in *Proceedings of International Workshop on Hadrons in Dense Matter*, (GSI, Darmstadt, 1997).
[53] M. Lutz, nucl-th/9709073.
[54] B. Hong, in *Proceedings of APCTP Workshop on Astro-Hadron Physics: Properties of Hadrons in Matter*, (World Scientific, Singapore, 1998).